ACS OMEGA

http://pubs.acs.org/journal/acsodf

Article

Effect of $\pi\cdots\pi$ Interactions of Donor Rings on Persistent Room-Temperature Phosphorescence in D_4–A Conjugates and Data Security Application

Harsh Bhatia, Suvendu Dey, and Debdas Ray*

Cite This: *ACS Omega* 2021, 6, 3858–3865

Read Online

ACCESS | Metrics & More | Article Recommendations | Supporting Information

ABSTRACT: Organic room-temperature phosphorescence (RTP) materials with persistent RTP (PRTP) have attracted huge interest in inks, bioimaging, and photodynamic therapy. However, the design principle to increase the lifetime of organic molecules is underdeveloped. Herein, we show donor(D_4)–acceptor(A) molecules (**TOEPh**, **TOCPh**, **TOMPh**, **TOF** and **TOPh**) with similar orientation of donor rings in aggregates that cause a large number of noncovalent interactions. We observed that **TOEPh**, **TOCPh**, **TOMPh** and **TOF** showed PRTP, whereas **TOPh** showed only phosphorescence emission (Φ_P = ∼11%) with no PRTP property at ambient conditions. The spectroscopic and single-crystal X-ray analyses confirm the molecular assembly via *J*-aggregation with a face-to-face orientation of the donor rings. The crystal structure analysis (**TOEPh**, **TOCPh**, **TOMPh**, **TOF**) reveals that moderate $\pi\cdots\pi$ interactions (3.706 to 4.065 Å) between the donor rings cause the enhancement of the phosphorescence lifetime (26 to 245 ms), whereas the short phosphorescence lifetime (12 ms) of **TOPh** was observed because of the absence of $\pi\cdots\pi$ interactions. We found that **TOEPh** shows a long lifetime (245 ms) as compared to other derivatives because of the presence of ethoxy (−OEt) groups that enables spin–orbit coupling caused by strong lone pair (O)$\cdots\pi$ interactions present in the molecule. Utilizing the PRTP feature of **TOEPh** and the fluorescence emission of **TOPh**, we have shown data security applications in poly(methyl methacrylate).

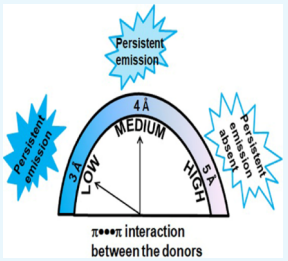

INTRODUCTION

Persistent room-temperature phosphorescence (PRTP) materials are emissive systems that show persistent luminescence characteristics, with the lifetime ranging from milliseconds (∼100 ms) to ∼20 min after switching off the excitation source.[1−5] Such PRTP materials find various applications in the field of security signs,[6,7] bioimaging,[8−10] molecular sensing,[11,12] and photodynamic therapy.[13,14] To this context, achieving RTP is a challenging task as it requires spin-forbidden intersystem crossing (ISC)[15,16] between the singlet (S) and triplet (T) states. Therefore, heavy metal-based phosphorescent materials[17,18] are generally used because of the strong spin–orbit coupling (SOC) induced by the heavy metals. However, these systems are highly expensive and toxic, which limit their practical applications. Recently, purely organic RTP materials have been extensively explored as they are cheaper and can be easily modified.[6,19−23] However, inefficient ISC caused by poor SOC between the S_n and T_n excited states leads to very low-emission quantum yields of the molecules, which prohibits their use in practical applications.[15,16,24,25] Additionally, thermal motion and energy transfer to oxygen molecules further contribute to the deactivation of triplet states, which leads to lower emission efficiency.[24,25] Considering these obstacles, organic molecular systems have been designed utilizing the concept of El-Sayed rule[15,26,27] that explains the S_n–T_n electron spin conversion in organic chromophores. According to the rule, the ISC rate will be higher when either $^1(n-\pi^*)$ to $^3(\pi-\pi^*)$ or $^1(\pi-\pi^*)$ to $^3(n-\pi^*)$ transitions are involved, but the transition is retarded when the orbitals involved are the same in configuration ($^1(n-\pi^*)$ to $^3(n-\pi^*)$ or $^1(\pi-\pi^*)$ to $^3(\pi-\pi^*)$).[15] Therefore, the incorporation of heteroatoms (O, N, and S), carbonyls, and cyano groups is commonly used in the organic molecules to favor ISC.[7,28−32] In combination with this strategy, rigid host–guest matrices,[33] crystallization,[34] aggregation,[35] and deuterium substitution[36] are the key design principles to suppress the nonradiative pathways that quench triplet states.

Self-assembly of the molecular system plays an important role in controlling the RTP behavior of the molecules at ambient conditions because of the increased intermolecular interactions that lock the molecular systems via controlled molecular packing and self-assembly of the molecules.[37−39] Despite the studies in the past, the precise and predetermined molecular structure arrangement is not optimized. The controlled molecular packing caused by a large number of intermolecular interactions plays an essential role in

Received: November 21, 2020
Accepted: January 15, 2021
Published: January 28, 2021

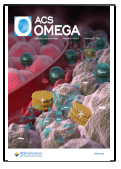

aggregation.[39,40] The aggregation of the molecules with an increased overlap of the π-clouds and a large number of noncovalent interactions can favor PRTP at ambient conditions.[41−43] Such intermolecular interactions lead to low ΔE_{ST} and a high rate of ISC, as recently suggested in the literature.[6,18,19,43] Introduction of H-bonding, C−H···π, N−H···π, C−H···O, and lone pair (lp)···π-cloud interactions in the aggregates complements the π···π interaction. Intra- and/or intermolecular interactions increase the rigidity of the molecular aggregates and stabilize the triplet states, which otherwise are prone to thermal motions like vibrations and rotations.[44,45] Therefore, the controlled assembly of the molecules with a large number of noncovalent interactions is a key to harness long persistent luminescence.[46−48] However, the molecular design principle that controls the orientation of the donor rings with the overlap of the π-cloud and noncovalent interactions is rare.[44,46,47,49,50] Taking a cue from our previous reports of D_4−A systems[6,19,51] in which the intramolecular interactions between the phenoxy donors have been effectively utilized to harness the triplet state, herein, we report five donor−acceptor (D_4−A) molecular systems (**TOPh**, **TOEPh**, **TOCPh**, **TOMPh** and **TOF**) (Figure 1) to

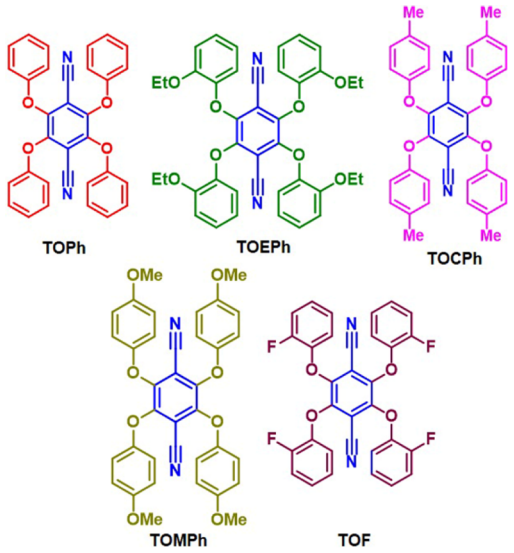

Figure 1. Molecular structures of **TOPh**, **TOEPh**, **TOCPh**, **TOMPh** and **TOF**.

understand the RTP quantum yield (Φ_P) with the persistent RTP characteristic utilizing intermolecular π···π interactions of the phenoxy donors. The molecules are designed to utilize the controlled arrangement of the substituted donor rings which impose steric and electronic effects to the molecular backbone. These molecular systems prefer to pack via intermolecular π···π (face-to-face)[46−48] interactions between the donor parts of the molecules, which suppress the nonradiative decay channels and enhance the triplet lifetimes.

The photophysical measurements of **TOPh**, **TOEPh** and **TOMPh** show dual phosphorescence band in the powder phase, whereas **TOCPh** shows a single phosphorescence emission band with a broad tail. The comparison of the phosphorescence lifetime measurements with the crystal structure reveals that persistent RTP features are observed for **TOEPh** and **TOMPh** because of the short intermolecular distance between the donor rings. However, **TOCPh** exhibits a longer phosphorescence lifetime as compared with **TOPh**. We found in comparison studies that only **TOPh**, which does not show intra- and/or intermolecular π···π interactions between the donor rings, displays a short RTP lifetime with a very high phosphorescence quantum yield of ∼11%, which otherwise is rare to be observed under ambient conditions (Table S1). Furthermore, all the molecular systems are likely to pack via J-aggregates that are responsible for the persistent emission feature. Finally, utilizing the afterglow feature, data encryption and decryption application is shown using the poly(methyl methacrylate) (PMMA) matrix.

RESULTS AND DISCUSSION

Absorption and Emission Studies. Figure 2 shows the normalized ultraviolet−visible (UV−vis) spectra of both

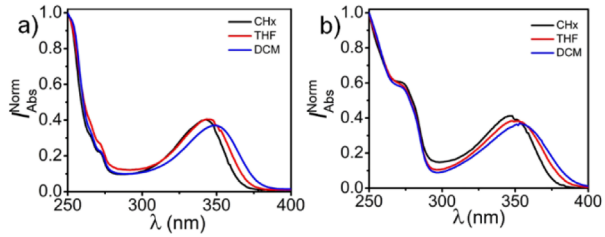

Figure 2. Absorption spectra of (a) **TOPh** and (b) **TOEPh** with disparate polarity of solvents.

TOPh and **TOEPh** in the solvents (10 μM) of disparate polarity. It can be seen that **TOEPh** exhibits a red-shifted absorption band at 355 nm as compared to **TOPh** (350 nm) in dichloromethane (DCM). Such red shift of the absorption band can be explained by the strong electron-donating group attached at the ortho positions of the phenoxy donors. The high-energy absorption bands at 280−290 nm of both the compounds are ascribed to the intramolecular π−π* transitions. However, the bathochromic shift of the absorption band (∼350 nm) with an increase in solvent polarity confirms that the ground state of both molecules has a charge transfer (CT) nature. Likewise, photoluminescence (PL) measurements were carried out in solvents of disparate polarity for both the molecules. The emission bands of **TOPh** were observed at 397, 403, and 411 nm when measured in cyclohexane (CHx), tetrahydrofuran (THF), and DCM, respectively, whereas **TOEPh** showed emission bands at 403 (CHx), 457 (THF), and 510 (DCM) nm (Figures 3 and S6). The bathochromic shift along with the reduced intensity of the emission spectra of both compounds in moving from nonpolar to polar solvents suggests the CT nature of the excited state. The large Stokes shift of 100 nm in **TOEPh** was observed because of the presence of strong electron-donating groups (−OEt). Moreover, the emission bands of **TOEPh** are more

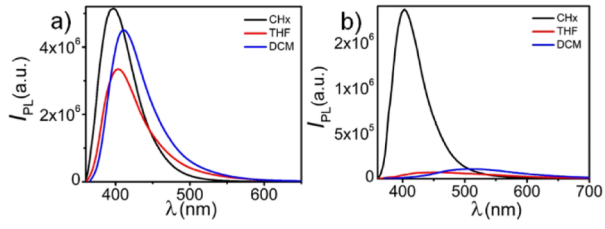

Figure 3. Steady-state emission spectra of (a) **TOPh** and (b) **TOEPh** in solutions. λ_{ex} = 365 nm.

https://dx.doi.org/10.1021/acsomega.0c05666
ACS Omega 2021, 6, 3858−3865

broad as compared to those of **TOPh**, thus suggesting the more relaxed excited states caused by solvent reorientation.

The steady-state emission spectra of both compounds in powder state show dual emission bands. **TOPh** shows a broad emission band at 410 nm along with a narrow emission at 485 nm, whereas **TOEPh** emits at 465 and 545 nm (Figures 4 and

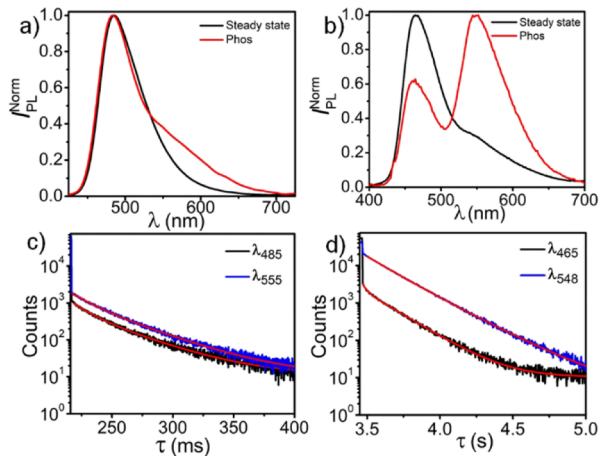

Figure 4. Steady-state and phosphorescence emission spectra of (a) **TOPh** and (b) **TOEPh** in powder. The phosphorescence decay of (c) **TOPh** and (d) **TOEPh**.

S7). The steady-state emission measurements at 77 K also show two emission bands in both molecules, as shown in Figure S7. **TOPh** emits at 400 and 480 nm, whereas relatively sharp emission bands at 460 and 555 nm are observed for **TOEPh**. The phosphorescence measurements of **TOPh** exhibit a narrow emission peak at 485 nm (τ_{485} = 12.94, 37.15 ms) along with a broad emission tail (535−700 nm) (τ_{555} = 15.19, 38.10 ms), whereas **TOEPh** shows two broad emission bands at 465 nm (τ_{465} = 26.42, 185.67 ms) and 548 nm (τ_{548} = 165.17, 245.82 ms) under ambient conditions (Figure 4). Similarly, at 77 K, both **TOPh** and **TOEPh** exhibit a well-resolved vibrational feature that is similar to the steady-state emission observed at 77 K. This indicates that the local triplet excited state contributes to the emission (Figure S7). The extended lifetimes of **TOEPh** (λ_{ex} = 370 nm) suggest the PRTP feature present in the system, whereas the relatively short lifetime of **TOPh** confirms that no persistent emission would be observed after switching off the excitation light source. Interestingly, the PL quantum yield (PLQY) of **TOEPh** (7.49%) was observed to be lower as compared to that of **TOPh** (36.6%). Such difference in the PLQY values can be explained by considering the molecular structure of both compounds. The low PLQY value of **TOEPh** is because of the presence of additional rotational channels caused by the O−C and C−C bonds of the ethoxy groups, which leads to an increase in the nonradiative deactivation channels and, hence, reduced emission efficiency.

Furthermore, the phosphorescence quantum yields of both the compounds were observed to be 10.97% (**TOPh**) and 6.96% (**TOEPh**), respectively. Such difference in the phosphorescence quantum yields (Φ_{Ph}) in both compounds suggests that relatively more nonradiative channels are involved in **TOEPh** as compared to that in **TOPh**. The long phosphorescence lifetime of **TOEPh** as compared to that of **TOPh** causes the excitons to dissipate their energy via various nonradiative deactivation pathways, such as triplet−triplet annihilation and energy transfer to the singlet oxygen.[24,25] Moreover, a large difference in the fluorescence quantum yield values of **TOPh** (Φ_{Fl} = 25.63%) and **TOEPh** (Φ_{Fl} = 0.53%) suggests that **TOEPh** has a relatively strong phosphorescence at ambient conditions. The additional lp of electrons of ethoxy groups at the ortho positions in **TOEPh** may favor ISC by an allowed transition between the $n-\pi^*$ and $\pi-\pi^*$ states, which is in good agreement with the literature[41] in which electronic coupling between the n and π units enables ISC transitions, thus resulting in strong RTP. Moreover, enhanced Φ_{Ph} of **TOEPh** confirms the indirect role of free electrons in quenching the fluorescence by favoring strong SOC. Finally, comparing the photophysical properties of both **TOEPh** and **TOPh,** we conclude that the presence of free lp of electrons in the ethoxy groups significantly affects the photophysical behavior of **TOEPh**. Therefore, molecular design with a trade-off between the extra lp of electrons and bulky alkyl chain may be used to switch the electronic properties of the organic luminescent molecules.

Single-Crystal X-Ray Analysis of TOPh and TOEPh. *Intramolecular Interactions.* In order to further understand the lifetimes of both the luminogens, we analyzed single-crystal X-ray structures in detail. The X-ray structures of both compounds (Figure 5) revealed that the phenoxy donors are covalently attached to the terephthalonitrile acceptor via the C−O single bond to give a twisted geometry. The orientation of the phenyl rings in **TOPh** and **TOEPh** is found to be alternatively above and below the plane of the terephthalonitrile core. The dihedral angles of the phenoxy rings in **TOPh**

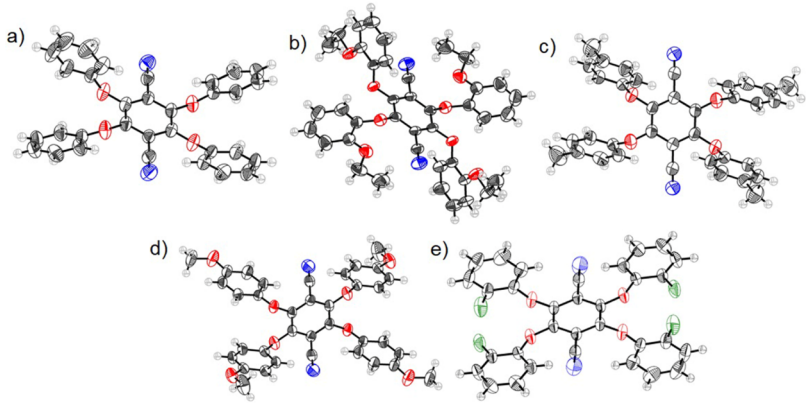

Figure 5. Crystal structure of (a) **TOPh**, (b) **TOEPh**, (c) **TOCPh**, (d) **TOMPh** and (e) **TOF**.

https://dx.doi.org/10.1021/acsomega.0c05666
ACS Omega 2021, 6, 3858−3865

are found to be 115.02, 129.60, 48.81, and 66.79° when viewed along the atoms C1−C2−O1−C9, C4−C3−O2−C15, C6−C5−O3−C21, and C5−C6−O4−C27, respectively. However, the dihedral angles in **TOEPh** are observed at 86.96 and 131.19° when viewed along the C1−C2−O1−C5 and C1−C3−O2−C11 atoms, respectively (Figure S8). Moreover, the centroid-to-centroid distance between the two intramolecular phenoxy rings was found to be 4.245 and 4.540 Å in **TOPh,** whereas it was found to be 5.302 Å in **TOEPh** (Figure S9). Such a long distance between the phenoxy rings along with their alternative up and down arrangement cause ineffective $\pi\cdots\pi$ overlap between the phenyl rings, alleviating the possibility of intramolecular through-space interactions between the rings. In addition, the angles between the planes of the phenoxy donors (**TOPh**: 21.77, 29.68°; **TOEPh**: 56.26°) are comparatively higher in the case of **TOEPh** (Figure S10), which further substantiate our previous line of argument.

In addition to this, a large number of strong lp$\cdots\pi$ interactions (2.729 Å, lp(O(2))$\cdots$C(4)≡N; 2.732 Å, lp(O(4))$\cdots\pi$(C_1=C_3); 2.778 Å, lp(O(1))$\cdots\pi$(C_4≡N); 2.902 Å, lp(O(1))$\cdots\pi$(C_{11}=C_{12}); 3.458 Å, lp(O(4))$\cdots\pi$(C_4≡N_1); 3.752 Å, lp(O(3))$\cdots\pi$(C_4≡N)) between the free electron pairs of ethoxy and phenoxy groups are found in **TOEPh**. We believe that these interactions not only reduce the rotation and vibrations of the donor rings but also cause the enhancement of ISC. In addition to this, intramolecular C−H$\cdots\pi$ interactions (2.947, 3.379, 3.538, 3.888 Å) are also present in **TOPh** as shown in Figure S11. When compared, similar interactions are also present in **TOPh** (2.708 Å, lp(O(3))$\cdots\pi$(C_8≡N); 2.708 Å, lp(O(2))$\cdots\pi$(C_8≡N); 2.730 Å, lp(O(1))$\cdots\pi$(C_7≡N); 2.726 Å, lp(O(4))$\cdots\pi$(C_7≡N); 3.157 Å, lp(O(3))$\cdots\pi$(C_{27}=C_{28}); 2.941 Å, lp(O(4))$\cdots\pi$(C_{21}=C_{22}); 2.993 Å, lp(O(1))$\cdots\pi$-(C_{15}=C_{16}); 3.181 Å, lp(O(2))$\cdots$(C_9=C_{10}); 2.594 Å, C−H(1)$\cdots\pi$); (2.648 Å, C−H(10)$\cdots\pi$); (2.0707 Å, C−H(11)$\cdots\pi$); (2.560 Å, C−H(20)$\cdots\pi$) (Figure S12). We anticipate that these large number of lp$\cdots\pi$ interactions significantly affect the photophysical properties of both molecular systems and certainly contribute to the strong ISC and longer lifetimes. Considering these large numbers of noncovalent interactions (lp(O)$\cdots\pi$, C−H$\cdots\pi$) that provide extra-stabilization of the triplet excited states by restricting the excited-state motion, we believe that nonradiative decay pathways are reduced significantly, leading to the extension of the lifetime in the millisecond range. Therefore, the presence of these intramolecular interactions plays a crucial role in populating the large number of ISC channels to harvest the triplet states. Although these intramolecular noncovalent interactions are present in both luminogens, only **TOEPh** displays pRTP,[52] suggesting such intramolecular interactions are not solely responsible for the enhancement of the RTP lifetime. To confirm the reason behind the long lifetime of **TOEPh**, we compared the intermolecular interactions present in both **TOPh** and **TOEPh**.

Intermolecular Interactions. The crystal structure analysis further shows that **TOPh** prefers to pack in slip-stack arrangement. The intermolecular distance (centroid to centroid) between the two terephthalonitrile rings is found to be 5.623 Å. However, such slip-stack arrangement is absent in the case of **TOEPh**. The steric hindrance imposed by ethoxy chains favor a large distance between the centroids of the two units (centroid to centroid: 7.760 Å) (Figure S13). These arrangements suggest that intermolecular centroid−centroid interactions between the acceptor units in both the molecular systems are lacking, unlocking the molecular motion in the excited state. The distance (π(C≡N)$\cdots\pi$−centroid−core) between the terephthalonitrile ring of one molecule and the nitrile group of another molecule in **TOPh** is observed at 3.815 and 3.769 Å (Figure S14). Interestingly, these interactions are absent in **TOEPh**. However, **TOEPh** that shows relatively shorter $\pi\cdots\pi$ interactions still possesses ∼7 times longer lifetime as compared to the former. Therefore, the longer phosphorescence lifetime of **TOEPh** as compared to that of **TOPh**[52] can be explained by the relatively shorter intermolecular $\pi\cdots\pi$ interactions between the phenoxy donors.[46,47] We conclude that intermolecular $\pi\cdots\pi$ interactions between the donor rings play a major role in the elongation of the triplet state lifetime, as these interactions immobilize the molecular motion in the excited state and reduce the nonradiative decay channels.[46,47]

Single-Crystal and Photophysical Studies of TOCPh and TOMPh. In order to further confirm the argument of $\pi\cdots\pi$ interactions that cause the enhancement of phosphorescence lifetime, we studied two more terephthalonitrile derivatives substituted with 4-methylphenoxy and 4-methoxyphenoxy donors. Similar to the other compounds, 2,3- and/or 5,6-positions of the terephthalonitrile core are angularly substituted with the phenoxy donors. The dihedral angles of the rings are found to be 64.40 and 80.77° in **TOCPh,** whereas **TOMPh** shows torsion of 57.62 and 82.03° when viewed along the C3−C2−O1−C5 and C2−C3−O2−C11 atoms, respectively (Figure S15). The lack of intramolecular face-to-face interactions between the phenoxy rings of **TOCPh** (centroid to centroid = 5.355 Å) and **TOMPh** (centroid to centroid = 5.193 Å) (Figure S16) further removes the possibility of intramolecular $\pi\cdots\pi$ interactions in these systems. Furthermore, strong intramolecular lp(O)$\cdots\pi$(C≡N) (**TOCPh**: O1$\cdots\pi$(C_4≡N_1), 2.797 Å; O2$\cdots\pi$(C_4≡N_1), 2.762 Å; **TOMPh**: O1$\cdots\pi$(C_4≡N_1), 2.789 Å; O2$\cdots\pi$(C_4≡N_1), 2.757 Å) (Figure S17) and lp(O)$\cdots\pi$(C=C) (**TOCPh**: O1$\cdots\pi$-(C_{11}=C_{12}), 3.235 Å; O2$\cdots\pi$(C_5=C_6), 2.968 Å; **TOMPh**: O1$\cdots\pi$(C_{11}=C_{12}), 3.275 Å, O2$\cdots\pi$(C_5=C_6), 2.893 Å) (Figure S18) interactions are also observed, which are very similar to that observed in both **TOPh** and **TOEPh**. In addition, multiple C−H$\cdots\pi$ interactions are also observed (**TOCPh**: 2.719, 2.514 Å; **TOMPh**: 2.745, 2.515 Å) (Figure S19). When we compared them with **TOPh**, the π(C≡N)$\cdots\pi$(C≡N) interactions (**TOCPh**: 4.293 Å; **TOMPh**: 4.376 Å) were also observed in both control molecules (Figure S20). However, the distance between the centroid of the terephthalonitrile core (acceptor) is found to be 7.863 Å (**TOCPh**) and 7.830 Å (**TOMPh**) (Figure S21). Such a large distance between the π-clouds of the acceptor rings (π(C≡N)$\cdots\pi$(C≡N) and $\pi\cdots\pi$ (acceptor)) in all the four molecular systems further confirms that acceptor−acceptor packing is not crucial in determining the increased phosphorescence lifetimes of all luminogens.

The presence of free lp of electrons on the oxygen atom of the phenoxy rings in **TOCPh** and **TOMPh** can contribute to the RTP feature because of the transition between the $n-\pi^*$ and $\pi-\pi^*$ states, as recently discussed in the literature.[6,7,19,30,31,41] We have performed solvent-dependent absorption and emission measurements at ambient conditions. Similar CT excited state characteristics of both molecules (**TOCPh** and **TOMPh**) are observed, as compared to that of earlier two molecules (**TOPh** and **TOEPh**) (Figure S6). The room-temperature steady-state emission measurements show a single emission band for both molecules (**TOCPh**, 481 nm;

https://dx.doi.org/10.1021/acsomega.0c05666
ACS Omega 2021, 6, 3858−3865

TOMPh, 480 nm). The lifetime analysis ensures that both **TOCPh** and **TOMPh** show long RTP emissions (λ_{ex} = 365 nm) (**TOCPh**: λ_{em} = 480 nm, τ_{480} = 35.39 ms, 72.00 ms; **TOMPh** λ_{em} = 480, τ_{480} = 64.01 ms, 108.70 ms; λ_{em} = 545 nm, τ_{545} = 69.45 ms, 130.68 ms; Figure S22). The low-temperature measurements at 77 K show that phosphorescence and steady-state emission closely overlap with each other with vibrational features, as shown in Figure S22. Such overlapping emission features also suggest that locally excited triplet state is present at 77 K. As the lifetimes of the molecules are very long, the possibility of triplet−triplet annihilation, energy transfer to oxygen, and triplet−triplet energy transfer may be responsible for the reduction of the quantum yield.[24,25] Along with this, the triplet exciton diffusion originating from the overlap of orbitals between the substituted phenoxy rings can substantially cause the quenching of the excitons, thus affecting the quantum yield.[53−55]

A significant difference in the lifetime values is observed for similarly packed molecular systems, as shown in Table 1. Both

Table 1. Photophysical and Crystal Data

molecules	$^a\lambda_{Phos}$ (nm)	$^b\tau_{Phos}$ (ms)	$\pi\cdots\pi$ interaction (Å)	$^a\Phi_{em}$ (%)	$^a\Phi_{Ph}$ (%)
TOPh	485	12.94 (23.08%), 37.15 (76.92%)	5.623	36.6	10.97
	555	15.19 (24.66%), 38.10 (75.34%)			
TOEPh	465	26.42 (6.06%), 185.67 (93.94%)	4.065	7.49	6.96
	548	165.17 (52.37%), 245.82 (47.63%)			
TOCPh	480	35.39 (71.54%), 72.00 (28.46%)	3.749	5.65	1.2
TOMPh	480	64.01 (42.25%), 108.7 (57.75%)	3.782	4.90	0.94
	545	69.45 (59.50%), 130.68 (40.50%)			
TOF	408	24.04 (39.82%), 88.77 (55.10%), 1.07 (5.08%)	3.706	3.86	0.8
	467	79.31 (38.41%), 33.88 (33.73%), 203.28 (27.86%)			

[a]Phosphorescence emission and quantum yields were measured under ambient condition (λ_{ex} = 365 nm). [b]Lifetimes were measured under ambient condition (λ_{ex} = 370 nm).

the **TOCPh** and **TOMPh** molecular systems pack in slip-stack arrangements similar to **TOPh**. Such a difference in the RTP lifetimes suggests that the slip-stack arrangement is not primarily responsible for the persistent emission in the molecules. Interestingly, the distances between the phenoxy donors are found to be 3.750 Å (**TOCPh**) and 3.782 Å (**TOMPh**) (Figure 6), which are very close, as compared to that of **TOPh**. Therefore, comparison among the lifetimes of all the molecules along with the intermolecular $\pi\cdots\pi$ interactions of the donors and loose packing of the π-acceptor core suggests that the orientation of the donor rings plays a major role in defining the extended lifetime of all the D_4−A molecular systems. It is clear that various intramolecular lp$\cdots\pi$ interactions lead to enable a large number of efficient ISC channels which populate the triplet state. In addition, these interactions restrict the reorganization of the molecular donor rings to some extent and stabilize the triplet excitons. The intermolecular $\pi\cdots\pi$ interactions between the donor rings

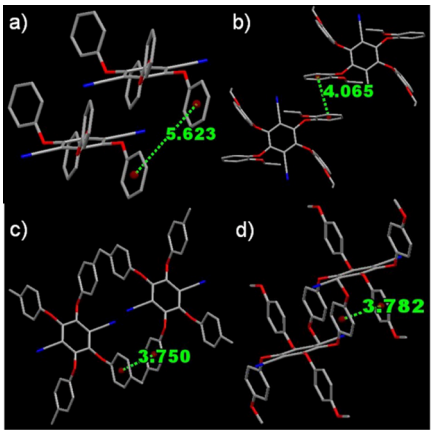

Figure 6. Distance between the centroids of the donor rings in (a) **TOPh** and (b) **TOEPh** (c) **TOCPh** and (d) **TOEPh**. Hydrogen atoms are omitted for clarity. Distances are measured in Å.

facilitate long PRTP by a further stabilization of the triplet states. Moreover, both intra- and/or intermolecular interactions are important to harness the triplet excitons efficiently. In the cases of **TOCPh** and **TOMPh,** the close arrangement of phenoxy rings (Table 1) leads to strong $\pi\cdots\pi$ interactions, which probably cause the efficient exciton migration and quench the triplet excitons.[24,53−55] Because of the exciton migration, the quantum yield of these molecules may be reduced, whereas in the case of **TOEPh,** strong $\pi\cdots\pi$ interactions are absent because of which the probability of exciton migration is reduced, and hence a high phosphorescence quantum yield is observed.[53] Taking all together, we can conclude that the terephthalonitrile core substituted by phenoxy rings leads to control the self-assembled molecular architecture with a large number of noncovalent interactions, which play a pivotal role in reducing the molecular motion and stabilizing the triplet states, hence long PRTP.

Effect of Aggregation. In order to check the effect of aggregation on PRTP, we collected the absorption spectra of all the molecules in THF and 90% (v/v) THF−H_2O mixture (Figures 7, S23). In THF, the lower energy absorption band

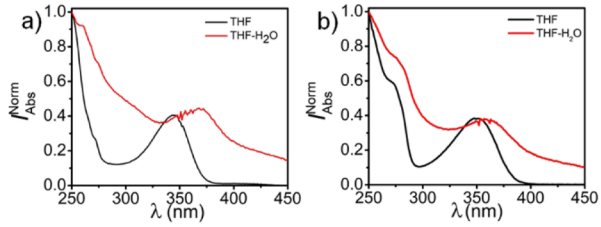

Figure 7. Absorption spectra of (a) **TOPh** and (b) **TOEPh** in THF and 90% (v/v) THF−H_2O.

was observed at 345 nm (**TOPh**), 350 (**TOEPh**) nm, 348 nm (**TOCPh**), and 355 nm (**TOMPh**) at a concentration of 10 mM under ambient condition. The addition of water leads to the turbidity of the solution which confirms the aggregate formation. When we compare the absorption spectra of all the chromophores with the aggregates, we found that the lower energy band was bathochromically shifted by 15−20 nm in all the molecules when recorded in a 90% THF−H_2O mixture. The red shift in the absorption spectra suggests the formation of *J*-aggregates. Contrary to the observed claim that H-

https://dx.doi.org/10.1021/acsomega.0c05666
ACS Omega 2021, 6, 3858−3865

aggregation causes the stabilization of triplet excited states and long persistent lifetime, *J*-aggregates in these molecular systems also cause the enhancement of the RTP lifetime. This observation further suggests that the type of aggregation plays no major role in determining the stabilization of the triplet excited states. Instead, the self-assembly of the molecules with a large number of intramolecular (lp$\cdots\pi$) and intermolecular $\pi\cdots\pi$ interactions are the determining factors in the enhancement of the phosphorescence lifetimes.[7,46−48] Moreover, we conclude that terephthalonitrile-based molecular systems are suitable to harness triplet excitons via face-to-face interaction between the donor phenoxy rings.

Effect of Electron-Withdrawing Group. The argument of donor-based face-to-face interaction was further confirmed by analyzing the crystal structure of the **TOF** molecule. **TOF** was chosen for comparison because it gives an afterglow emission at 465 nm with a maximum lifetime of 203.28 ms (Figure S24). The complete photophysical data of **TOF** can be obtained from the earlier report.[6] When the crystal structure of **TOF** was compared with that of **TOPh**, **TOEPh**, **TOCPh** and **TOMPh** we observed that **TOF** also packs via slip-stack arrangement. The distance between the core terephthalonitrile rings is found to be very large (7.513 Å), whereas a short distance (3.706 Å) is observed for the intermolecular phenoxy donor rings (Figure S25). Such a short distance between the π-clouds confirms that $\pi\cdots\pi$ interaction (intermolecular) is the major reason which governs the extended lifetime in this class of terephthalonitrile-based derivatives.

Persistent RTP Feature and Data Security Application in PMMA-Doped Films. The PRTP feature in the powder samples of **TOPh**, **TOEPh**, **TOCPh** and **TOMPh** is shown in Figure 8a. Utilizing the PRTP feature of **TOEPh** and the short

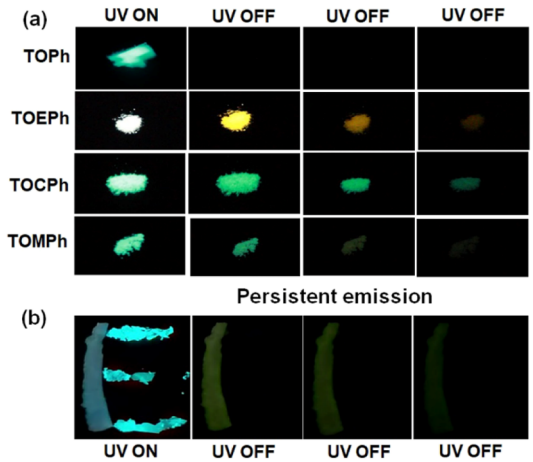

Figure 8. (a) PRTP feature of **TOPh**, **TOEPh**, **TOCPh** and **TOMPh** in powder under ambient conditions. (b) Data security application patterns of "E" and "I" under illumination with a 365 nm lamp using the PMMA films of **TOPh** and **TOEPh**.

phosphorescence lifetime of **TOPh**, we have shown the encryption and decryption application using both the molecules in the PMMA-doped films (Figure 8b). Under 365 nm illumination, the pattern of "E" made of both **TOEPh** and **TOPh** with different emission features was observed. On switching off the excitation source, only a green pattern of "I" caused by **TOEPh** shows a persistent emission feature that could be readily visualized by naked eye.

CONCLUSIONS

In summary, we have compared five terephthalonitrile derivatives, **TOPh**, **TOEPh**, **TOCPh**, **TOMPh,** and **TOF,** in which the 2,3,5,6-positions are covalently attached with phenoxy, 2-ethoxyphenoxy, 4-methylphenoxy, 4-methoxyphenoxy, and 2-fluorophenoxy groups, respectively. We have shown that all the molecular systems show RTP features. Because of the presence of a large number of lp(O)$\cdots\pi$ intramolecular interactions, all the molecules favor a strong ISC that leads to triplet emission. Spectroscopic measurements and a detailed single-crystal X-ray structure analysis show that intermolecular $\pi\cdots\pi$ interactions between the donor rings play a major role in the enhancement of phosphorescence lifetime in **TOEPh**, **TOCPh**, **TOMPh** and **TOF**. Our results demonstrate that all the molecules assemble via J-aggregation but show a longer lifetime, which is against the generally proven hypothesis of triplet state stabilization by H-aggregates. We assume that terephthalonitrile-based derivatives provide the required assembly of the molecular systems with face-to-face donor interactions, which causes the elongation of the lifetime. Given the PRTP property of the molecules, data security application has been shown. Further studies and molecular engineering of this class of molecular systems to enhance the phosphorescence efficiency are underway.

EXPERIMENTAL SECTION

Materials and Measurements. All the reagents and deuterated solvents were obtained from commercial sources and used without any further purification, unless otherwise mentioned. Dimethyl formamide (DMF) was dried and distilled over calcium hydride. ^{1}H and ^{13}C NMR spectra were recorded in a Bruker AVHDN 400 with working frequencies of 400.245 MHz for ^{1}H and 100.6419 MHz for ^{13}C nuclei, respectively, using $CDCl_3$ and DMSO-d_6. Chemical shifts were quoted in ppm relative to tetramethylsilane, using the residual solvent peak as a reference standard. Steady-state absorbance was measured using an Agilent Technologies Cary 8454 UV−visible (vis) instrument. Steady-state emission, phosphorescence, and lifetime analysis of both fluorescence and phosphorescence were recorded on a HORIBA Fluorolog-3 spectrofluorometer (Model: FL3-2-IHR320). The phosphorescence spectra were recorded by giving the detector a delay of 50 μs (at room temperature and 1 ms at 77 K) and providing the sample window 3 times the lifetime of phosphor. Absolute quantum yield measurements of the compounds in solid state were recorded by using an integrating sphere purchased from HORIBA Jobin Yvon (Quanta-Phi 6, Model F-3029). Single-crystal X-ray diffraction data were collected using a D8 VENTURE IμS microfocus dual source Bruker APEX3 diffractometer equipped with a PHOTON 100 CMOS detector and an Oxford cryogenic system. High-performance liquid chromatography experiments were carried out on a Waters Alliance system (Milford, MA) consisting of an e2695 separation module and a 2998 photodiode array detector. Matrix-assisted laser desorption ionization (MALDI) measurements were performed with a Bruker autoflex maX MALDI mass spectrometer (equipped with Bruker smart beam-II laser), and data were measured in reflector positive mode. Detailed synthesis of all the molecules can be found in the Supporting Information..

https://dx.doi.org/10.1021/acsomega.0c05666
ACS Omega 2021, 6, 3858−3865

■ ASSOCIATED CONTENT

Supporting Information

The Supporting Information is available free of charge at https://pubs.acs.org/doi/10.1021/acsomega.0c05666.

Experimental procedures; NMR spectra; single-crystal X-ray diffraction analysis; UV−vis absorption spectra; steady-state emission; time-correlated single photon counting; phosphorescence measurement; RTP properties of **TOPh**, **TOEPh**, **TOCPh**, and **TOMPh**; **TOF** in powder; and photophysical properties including lifetimes, emission spectra, and absolute quantum yields (PDF)

Crystallographic data for TOPh (CIF)

Crystallographic data for **TOEPh** (CIF)

Crystallographic data for **TOCPh** (CIF)

Crystallographic data for **TOMPh** (CIF)

■ AUTHOR INFORMATION

Corresponding Author

Debdas Ray − *Advanced Photofunctional Materials Laboratory, Department of Chemistry, Shiv Nadar University, Gautam Buddha Nagar 201314, Uttar Pradesh, India;* orcid.org/0000-0002-6169-8823; Email: debdas.ray@snu.edu.in

Authors

Harsh Bhatia − *Advanced Photofunctional Materials Laboratory, Department of Chemistry, Shiv Nadar University, Gautam Buddha Nagar 201314, Uttar Pradesh, India*

Suvendu Dey − *Advanced Photofunctional Materials Laboratory, Department of Chemistry, Shiv Nadar University, Gautam Buddha Nagar 201314, Uttar Pradesh, India*

Complete contact information is available at: https://pubs.acs.org/10.1021/acsomega.0c05666

Notes

The authors declare no competing financial interest.

■ ACKNOWLEDGMENTS

D.R. is grateful to the Science & Engineering Research Board (SERB) (file no: EEQ/2020/000029), DST; Board of Research and Nuclear Science (BRNS) (file no. 37(3)/14/08-2018-BRNS/37130), DAE; H.B. thanks SNU for fellowship.

■ REFERENCES

(1) Kabe, R.; Adachi, C. Organic Long Persistent Luminescence. *Nature* **2017**, *550*, 384−387.

(2) Wang, Z.; Zhang, Y.; Wang, C.; Zheng, X.; Zheng, Y.; Gao, L.; Yang, C.; Li, Y.; Qu, L.; Zhao, Y. Color-Tunable Polymeric Long-Persistent Luminescence Based on Polyphosphazenes. *Adv. Mater.* **2020**, *32*, 1907355.

(3) Jin, J.; Jiang, H.; Yang, Q.; Tang, L.; Tao, Y.; Li, Y.; Chen, R.; Zheng, C.; Fan, Q.; Zhang, K. Y.; Zhao, Q.; Huang, W. Thermally Activated Triplet Exciton Release for Highly Efficient Tri-Mode Organic Afterglow. *Nat. Commun.* **2020**, *11*, 842.

(4) Nishimura, N.; Lin, Z.; Jinnai, K.; Kabe, R.; Adachi, C. Many Exciplex Systems Exhibit Organic Long-Persistent Luminescence. *Adv. Funct. Mater.* **2020**, *30*, 2000795.

(5) Zhang, T.; Ma, X.; Wu, H.; Zhu, L.; Zhao, Y.; Tian, H. Molecular Engineering for Metal-Free Amorphous Materials with Room-Temperature Phosphorescence. *Angew. Chem., Int. Ed.* **2020**, *59*, 11206−11216.

(6) Bhatia, H.; Ray, D. Use of Dimeric Excited States of the Donors in D_4-A Systems for Accessing White Light Emission, Afterglow, and Invisible Security Ink. *J. Phys. Chem. C* **2019**, *123*, 22104−22113.

(7) Chen, X.; Liu, Z.-F.; Jin, W. J. The Effect of Electron Donation and Intermolecular Interactions on Ultralong Phosphorescence Lifetime of 4-Carnoyl Phenylboronic Acids. *J. Phys. Chem. A* **2020**, *124*, 2746−2754.

(8) Zhi, J.; Zhou, Q.; Shi, H.; An, Z.; Huang, W. Organic Room Temperature Phosphorescence Materials for Biomedical Applications. *Chem.—Asian J.* **2020**, *15*, 947−957.

(9) Shi, H.; Zou, L.; Huang, K.; Wang, H.; Sun, C.; Wang, S.; Ma, H.; He, Y.; Wang, J.; Yu, H.; Yao, W.; An, Z.; Zhao, Q.; Huang, W. A Highly Efficient Red Metal-Free Organic Phosphor for Time-Resolved Luminescence Imaging and Photodynamic Therapy. *ACS Appl. Mater. Interfaces* **2019**, *11*, 18103−18110.

(10) Chen, X.; Xu, C.; Wang, T.; Zhou, C.; Du, J.; Wang, Z.; Xu, H.; Xie, T.; Bi, G.; Jiang, J.; Zhang, X.; Demas, J. N.; Trindle, C. O.; Luo, Y.; Zhang, G. Versatile Room-Temperature-Phosphorescent Materials Prepared from N-Substituted Naphthalimides: Emission Enhancement and Chemical Conjugation. *Angew. Chem., Int. Ed.* **2016**, *55*, 9872−9876.

(11) Yu, X.; Liang, W.; Huang, Q.; Wu, W.; Chruma, J. J.; Yang, C. Room-Temperature Phosphorescent γ-Cyclodextrin-Cucurbit[6]Uril-Cowheeled [4]Rotaxanes for Specific Sensing of Tryptophan. *Chem. Commun.* **2019**, *55*, 3156−3159.

(12) Hoshi, M.; Nishiyabu, R.; Hayashi, Y.; Yagi, S.; Kubo, Y. Room-Temperature Phosphorescence-Active Boronate Particles: Characterization and Ratiometric Afterglow-Sensing Behavior by Surface Grafting of Rhodamine B. *Chem.—Asian J.* **2020**, *15*, 787−795.

(13) Xu, L.; Zhou, K.; Ma, H.; Lv, A.; Pei, D.; Li, G.; Zhang, Y.; An, Z.; Li, A.; He, G. Ultralong Organic Phosphorescent Nanocrystals with Long-Lived Triplet Excited States for Afterglow Imaging and Photodynamic Therapy. *ACS Appl. Mater. Interfaces* **2020**, *12*, 18385−18394.

(14) Zhen, X.; Qu, R.; Chen, W.; Wu, W.; Jiang, X. Development of Phosphorescent Probes for in Vitro and in Vivo Bioimaging. *Biomater. Sci.* **2020**, *9*, 285−300, DOI: 10.1039/D0BM00819B.

(15) Turro, N. J.; Ramamurthy, V.; Scaiano, J. C. *Principles of Molecular Photochemistry : An Introduction*; University Science Books: Sausalito, California, 2009.

(16) Baryshnikov, G.; Minaev, B.; Ågren, H. Theory and Calculation of the Phosphorescence Phenomenon. *Chem. Rev.* **2017**, *117*, 6500−6537.

(17) Fan, C.; Yang, C. Yellow/Orange Emissive Heavy-Metal Complexes as Phosphors in Monochromatic and White Organic Light-Emitting Devices. *Chem. Soc. Rev.* **2014**, *43*, 6439−6469.

(18) Ravotto, L.; Ceroni, P. Aggregation Induced Phosphorescence of Metal Complexes: From Principles to Applications. *Coord. Chem. Rev.* **2017**, *346*, 62−76.

(19) Bhatia, H.; Bhattacharjee, I.; Ray, D. Biluminescence via Fluorescence and Persistent Phosphorescence in Amorphous Organic Donor(D_4)-Acceptor(A) Conjugates and Application in Data Security Protection. *J. Phys. Chem. Lett.* **2018**, *9*, 3808−3813.

(20) Alam, P.; Leung, N. L. C.; Liu, J.; Cheung, T. S.; Zhang, X.; He, Z.; Kwok, R. T. K.; Lam, J. W. Y.; Sung, H. H. Y.; Williams, I. D.; Chan, C. C. S.; Wong, K. S.; Peng, Q.; Tang, B. Z. Two Are Better Than One: A Design Principle for Ultralong-Persistent Luminescence of Pure Organics. *Adv. Mater.* **2020**, *32*, 2001026.

(21) Bhattacharjee, I.; Acharya, N.; Bhatia, H.; Ray, D. Dual Emission through Thermally Activated Delayed Fluorescence and Room-Temperature Phosphorescence, and Their Thermal Enhancement via Solid-State Structural Change in a Carbazole-Quinoline Conjugate. *J. Phys. Chem. Lett.* **2018**, *9*, 2733−2738.

(22) Bhattacharjee, I.; Acharya, N.; Karmakar, S.; Ray, D. Room-Temperature Orange-Red Phosphorescence by Way of Intermolecular Charge Transfer in Single-Component Phenoxazine−Quinoline

Conjugates and Chemical Sensing. *J. Phys. Chem. C* **2018**, *122*, 21589−21597.
(23) Bhattacharjee, I.; Acharya, N.; Ray, D. Thermally Activated Delayed Fluorescence and Room-Temperature Phosphorescence in Naphthyl Appended Carbazole−Quinoline Conjugates, and Their Mechanical Regulation. *Chem. Commun.* **2019**, *55*, 1899−1902.
(24) Hirata, S. Recent Advances in Materials with Room-Temperature Phosphorescence: Photophysics for Triplet Exciton Stabilization. *Adv. Opt. Mater.* **2017**, *5*, 1700116.
(25) Hirata, S. Ultralong-Lived Room Temperature Triplet Excitons: Molecular Persistent Room Temperature Phosphorescence and Nonlinear Optical Characteristics with Continuous Irradiation. *J. Mater. Chem. C* **2018**, *6*, 11785−11794.
(26) Lower, S. K.; El-Sayed, M. A. The Triplet State and Molecular Electronic Processes in Organic Molecules. *Chem. Rev.* **1966**, *66*, 199−241.
(27) El-Sayed, M. A. Spin-Orbit Coupling and the Radiationless Processes in Nitrogen Heterocyclics. *J. Chem. Phys.* **1963**, *38*, 2834−2838.
(28) Baroncini, M.; Bergamini, G.; Ceroni, P. Rigidification or Interaction-Induced Phosphorescence of Organic Molecules. *Chem. Commun.* **2017**, *53*, 2081−2093.
(29) Shimizu, M.; Nagano, S.; Kinoshita, T. Dual Emission from Precious Metal-Free Luminophores Consisting of C, H, O, Si, and S/P at Room Temperature. *Chem.—Eur. J.* **2020**, *26*, 5162−5167.
(30) Jia, X.; Yue, B.; Zhou, L.; Niu, X.; Wu, W.; Zhu, L. Fluorescence to Multi-Colored Phosphorescence Interconversion of a Novel, Asterisk-Shaped Luminogen via Multiple External Stimuli. *Chem. Commun.* **2020**, *56*, 4336−4339.
(31) Zheng, S.; Hu, T.; Bin, X.; Wang, Y.; Yi, Y.; Zhang, Y.; Yuan, W. Z. Clustering-Triggered Efficient Room-Temperature Phosphorescence from Nonconventional Luminophores. *ChemPhysChem* **2020**, *21*, 36−42.
(32) Yuan, J.; Wang, Y.; Li, L.; Wang, S.; Tang, X.; Wang, H.; Li, M.; Zheng, C.; Chen, R. Activating Intersystem Crossing and Aggregation Coupling by CN-Substitution for Efficient Organic Ultralong Room Temperature Phosphorescence. *J. Phys. Chem. C* **2020**, *124*, 10129−10134.
(33) Fang, W. J.; Zhang, J. J.; Zhao, H.; Ni, J.; Liu, S. Q.; Liu, Z.; Ni, A. Y.; Zhang, P. P.; Wei, H. H. Versatile Induction of Efficient Organic-Based Room-Temperature Phosphorescence via Al-DMSO Matrices Encapsulation. *Adv. Opt. Mater.* **2020**, *8*, 2000482.
(34) He, G.; Du, L.; Gong, Y.; Liu, Y.; Yu, C.; Wei, C.; Yuan, W. Z. Crystallization-Induced Red Phosphorescence and Grinding-Induced Blue-Shifted Emission of a Benzobis(1,2,5-Thiadiazole)−Thiophene Conjugate. *ACS Omega* **2019**, *4*, 344−351.
(35) Sudhakar, P.; Radhakrishnan, T. P. Stimuli Responsive and Reversible Crystalline−Amorphous Transformation in a Molecular Solid: Fluorescence Switching and Enhanced Phosphorescence in the Amorphous State. *J. Mater. Chem. C* **2019**, *7*, 7083−7089.
(36) Watts, R. J.; Strickler, S. J. Deuterium Isotope Effects on the Lifetime of the Phosphorescent Triplet State of Naphthalene. *J. Chem. Phys.* **1968**, *49*, 3867−3871.
(37) Wu, T.; Huang, J.; Yan, Y. Self-Assembly of Aggregation-Induced-Emission Molecules. *Chem.—Asian J.* **2019**, *14*, 730−750.
(38) Wu, H.; Hang, C.; Li, X.; Yin, L.; Zhu, M.; Zhang, J.; Zhou, Y.; Ågren, H.; Zhang, Q.; Zhu, L. Molecular Stacking Dependent Phosphorescence−Fluorescence Dual Emission in a Single Luminophore for Self-Recoverable Mechanoconversion of Multicolor Luminescence. *Chem. Commun.* **2017**, *53*, 2661−2664.
(39) Li, Q.; Li, Z. Molecular Packing: Another Key Point for the Performance of Organic and Polymeric Optoelectronic Materials. *Acc. Chem. Res.* **2020**, *53*, 962−973.
(40) Jia, W.; Wang, Q.; Shi, H.; An, Z.; Huang, W. Manipulating the Ultralong Organic Phosphorescence of Small Molecular Crystals. *Chem.—Eur. J.* **2020**, *26*, 4437−4448.
(41) Yang, Z.; Mao, Z.; Zhang, X.; Ou, D.; Mu, Y.; Zhang, Y.; Zhao, C.; Liu, S.; Chi, Z.; Xu, J.; Wu, Y.-C.; Lu, P.-Y.; Lien, A.; Bryce, M. R. Intermolecular Electronic Coupling of Organic Units for Efficient Persistent Room-Temperature Phosphorescence. *Angew. Chem., Int. Ed.* **2016**, *55*, 2181−2185.
(42) Sutton, C.; Risko, C.; Brédas, J.-L. Noncovalent Intermolecular Interactions in Organic Electronic Materials: Implications for the Molecular Packing vs Electronic Properties of Acenes. *Chem. Mater.* **2016**, *28*, 3−16.
(43) Yang, Z.; Ubba, E.; Huang, Q.; Mao, Z.; Li, W.; Chen, J.; Zhao, J.; Zhang, Y.; Chi, Z. Enabling Dynamic Ultralong Organic Phosphorescence in Molecular Crystals through the Synergy between Intramolecular and Intermolecular Interactions. *J. Mater. Chem. C* **2020**, *8*, 7384−7392.
(44) Wen, Y.; Liu, H.; Zhang, S.; Gao, Y.; Yan, Y.; Yang, B. One-Dimensional $\pi-\pi$ Stacking Induces Highly Efficient Pure Organic Room-Temperature Phosphorescence and Ternary-Emission Single-Molecule White Light. *J. Mater. Chem. C* **2019**, *7*, 12502−12508.
(45) Bian, L.; Shi, H.; Wang, X.; Ling, K.; Ma, H.; Li, M.; Cheng, Z.; Ma, C.; Cai, S.; Wu, Q.; Gan, N.; Xu, X.; An, Z.; Huang, W. Simultaneously Enhancing Efficiency and Lifetime of Ultralong Organic Phosphorescence Materials by Molecular Self-Assembly. *J. Am. Chem. Soc.* **2018**, *140*, 10734−10739.
(46) Gan, N.; Wang, X.; Ma, H.; Lv, A.; Wang, H.; Wang, Q.; Gu, M.; Cai, S.; Zhang, Y.; Fu, L.; Zhang, M.; Dong, C.; Yao, W.; Shi, H.; An, Z.; Huang, W. Manipulating the Stacking of Triplet Chromophores in the Crystal Form for Ultralong Organic Phosphorescence. *Angew. Chem., Int. Ed.* **2019**, *58*, 14140−14145.
(47) Liu, W.; Wang, J.; Gong, Y.; Liao, Q.; Dang, Q.; Li, Z.; Bo, Z. Room-Temperature Phosphorescence Invoked Through Norbornyl-Driven Intermolecular Interaction Intensification with Anomalous Reversible Solid-State Photochromism. *Angew. Chem., Int. Ed.* **2020**, *59*, 20161−20166.
(48) Yamada, M.; Ishigaki, K.; Taniguchi, T.; Karatsu, T. Persistent Room Temperature Blue Phosphorescence from Racemic Crystals of 1,1-Diphenylmethanol Derivatives. *J. Photochem. Photobiol., A* **2021**, *407*, 113043.
(49) Yang, J.; Zhen, X.; Wang, B.; Gao, X.; Ren, Z.; Wang, J.; Xie, Y.; Li, J.; Peng, Q.; Pu, K.; Li, Z. The Influence of the Molecular Packing on the Room Temperature Phosphorescence of Purely Organic Luminogens. *Nat. Commun.* **2018**, *9*, 840.
(50) Chai, Z.; Wang, C.; Wang, J.; Liu, F.; Xie, Y.; Zhang, Y.-Z.; Li, J.-R.; Li, Q.; Li, Z. Abnormal Room Temperature Phosphorescence of Purely Organic Boron-Containing Compounds: The Relationship between the Emissive Behaviorand the Molecular Packing, and the Potential Related Applications. *Chem. Sci.* **2017**, *8*, 8336−8344.
(51) Bhatia, H.; Ray, D. Asymmetric-Donor (D_2D_2')−Acceptor(A) Conjugates for Simultaneously Accessing Intrinsic Blue-RTP and Blue-TADF. *Mater. Adv.* **2020**, *1*, 1858−1865.
(52) Zhao, W.; He, Z.; Lam, J. W. Y.; Peng, Q.; Ma, H.; Shuai, Z.; Bai, G.; Hao, J.; Tang, B. Z. Rational Molecular Design for Achieving Persistent and Efficient Pure Organic Room-Temperature Phosphorescence. *Chem.* **2016**, *1*, 592−602.
(53) Narushima, K.; Kiyota, Y.; Mori, T.; Hirata, S.; Vacha, M. Suppressed Triplet Exciton Diffusion Due to Small Orbital Overlap as a Key Design Factor for Ultralong-Lived Room-Temperature Phosphorescence in Molecular Crystals. *Adv. Mater.* **2019**, *31*, 1807268.
(54) Wang, Y.; Zhang, W.; Li, Y.; Ye, L.; Yang, G. X-Ray Crystal Structure of Gallium Tris-(8-Hydroxyquinoline): Intermolecular π - π Stacking Interactions in the Solid State. *Chem. Mater.* **1999**, *11*, 530−532.
(55) Hirata, S. Roles of Localized Electronic Structures Caused by π Degeneracy Due to Highly Symmetric Heavy Atom-Free Conjugated Molecular Crystals Leading to Efficient Persistent Room-Temperature Phosphorescence. *Adv. Sci.* **2019**, *6*, 1970085.

https://dx.doi.org/10.1021/acsomega.0c05666
ACS Omega 2021, 6, 3858−3865